geosciences

Article

Impact of the Hydrogeological Conditions on the Calculated Surface Uplift above Abandoned and Flooded Coal Mines

Andre Vervoort

Department of Civil Engineering, KU Leuven, 3000 Leuven, Belgium; andre.vervoort@kuleuven.be; Tel.: +32-163-211-71

Abstract: Upward surface movement or uplift has been extensively observed above abandoned and flooded deep coal mines, which used the longwall mining method, i.e., a caving method. Detailed analysis of satellite measurements indicated that the process of uplift is one of the more complex phenomena in ground control. The observed uplift is linked to the flooding of the underground infrastructure and rock mass. This was confirmed by conducting analytical calculations. The distribution of water pressure at the end of the mining phase and their increase during the flooding is an important aspect in all estimations. The main objectives of the study are to compare the impact of various hydrogeological conditions of this distribution at the start of the flooding phase and to select the most realistic one. They range from a zero-water pressure to a linear decrease from the top to the bottom longwall panel. Different scenarios of how the water pressures change as a function of time are also compared, i.e., from filling an open reservoir from bottom to top, to a systematic change in the linear downward trend. The main conclusion is that a linear trend, i.e., the original assumed scenario, is the best option in comparison to the other scenarios evaluated. It provides the best fit between the estimated uplift values and the large amount of remote sensing measurements along north–south transects in the Belgian Campine coal basin.

Keywords: flooded coal mines; abandoned coal mines; longwall; ground control; surface movement; uplift; analytical calculations

check for updates

Citation: Vervoort, A. Impact of the Hydrogeological Conditions on the Calculated Surface Uplift above Abandoned and Flooded Coal Mines. *Geosciences* **2022**, *12*, 454. https://doi.org/10.3390/geosciences12120454

Academic Editors: Mohamed Shahin and Jesus Martinez-Frias

Received: 19 September 2022
Accepted: 10 December 2022
Published: 14 December 2022

1. Introduction

Underground mining, and more specifically when using a total extraction mining method such as longwall mining, has a significant impact on the environment. Above the deep coal mines in the Campine coal district, Belgium, downward surface movements or subsidence of the order of several meters occurred, even at some locations more than 10 m. Such large movements have, among others, an impact on the surface water and on the hydrological situation above and around the mined zones. For example, dikes had to be constructed and systematically raised to restrain the water within the river and canal courses [1], and permanent pumping is needed to prevent the flooding of some surface areas. When applying the longwall mining method in a coal mine, one excavates one or more coal seams over large areas. The coal seam is divided up in individual longwall panels. Typical dimensions of the panels in the Campine coal district were 200 m on 800 m. As in the excavated areas, no support is present, and the first layers of the roof above each excavated coal seam collapse. Due to the mechanical swelling or expansion of the collapsed roof blocks, the goaf (i.e., the volume of collapsed blocks) fills the mining height, plus the height of the collapsed roof layers. Hence, the goaf starts to act as a regional support to the overlaying coal strata.

At the end of last century, the mining activities in several European coal districts were stopped, and the underground facilities were abandoned. This was followed by the flooding of the underground, i.e., both the infrastructure and the rock mass. The latter comprises goaf material, fractured and damaged rock, and intact but deformed strata.

The main impact of this flooding was the start of upward surface movement above and around the mined areas, e.g., [2–9]. In the Campine coal district, the uplift phase of the surface movement has not stopped yet, about 30 years after the mine closure [10]. However, the total amount of uplift is estimated to be—generally speaking—an order of magnitude smaller than the total amount of subsidence. In other words, there are areas where the total uplift will finally reach half to one meter. It is important to note that the ratio between total subsidence and total uplift is not a fixed ratio, but it varies over the mined zone and its surrounding [11]. The study of the uplift is important as also during this phase of surface movement, damage is induced to buildings and infrastructure [12]. It is also critical to know how long the impact of underground mining will last [10].

In the period around the mine closure in European coal districts, the remote sensing technique, based on satellite images, became more accessible for research [4]. This allowed the observation of surface movements over large areas and over long time periods. Hence, these techniques have now become an important observation and measurement tool, e.g., [13–16]. For this study, the European C-band ERS1/2 data and the ENVISAT-ASAR data were analyzed.

Although the extensive number of measurements clearly quantifies the uplift above abandoned coal mines, there is a need to understand the complex process of uplift and the link with the flooding of the underground infrastructure and rock mass. This is a real challenge, and one should look at various aspects. In 2021, an analytical framework was published [17], providing a good correlation between measured and calculated values. In this paper, the focus is on an evaluation of various possible hydrogeological scenarios and their impact on the estimated uplift above the abandoned and flooded coal mine of Eisden, Belgium. The distribution of water pressures at the end of the mining phase and their increase during the flooding are hereby important aspects in all estimations. Various hydrogeological conditions of this distribution at the start of the flooding phase are compared using the analytical framework (see further for details). They range from a zero-water pressure to a linear decrease from the top to the bottom longwall panel. Various scenarios of how the water pressures change as a function of time are also compared, i.e., from filling an open reservoir from bottom to top, to a systematic change in the linear downward trend.

The calculated uplift values for the various scenarios are compared to the satellite data. The original assumed scenario, i.e., a linear trend, remains the most likely option. It provides the best fit between the estimated uplift values and the large amount of remote sensing measurements along north–south transects in the Belgian Campine coal basin.

2. Overview of Past Studies on the Surface Uplift in the Campine Coal District, Belgium

One cannot overestimate the complexity of the process of uplift and the link between the flooding and the uplift of the earth surface. Numerous mining, geotechnical, geological, and hydrological conditions determine, in one way or another, the amount of uplift at a specific location. Hence, one must always work site specific. Due to the complexity of the process of uplift, the main aim of the studies rather is to better understand the process than to predict the amount of uplift. Of course, the latter should be the final aim.

At the end of 2021, a double paper was published on the surface movement above one coal mine of the Campine coal district in Belgium, i.e., the Eisden coal mine [1,17]. The Part A paper discusses in detail the remote sensing measurements by satellites (InSAR, Interferometry with Synthetic Aperture Radar data), while the companion Part B paper presents a framework to calculate analytically the amount of uplift. The latter allows an easy comparison of various scenarios and assumptions, which helps to understand the phenomenon. For details on the analysis of the measurements and on the proposed analytical framework, I refer the reader to this double paper, including references to research by others.

The main conclusion of the analysis of the InSAR data was that a large variation is observed both as a function of space and of time [1]. In other words, one cannot summarize the uplift by a single value or trend. The coal mine was closed in 1988 and, from October 1992 onwards, uplift was clearly visible above the mined zone. However, uplift also is observed away from the mined zone. The extent of uplift is at the start of the uplift phase situated in the central part and not at the boundaries of the mined zone. In Figure 1, the amount of uplift in two observation periods along a north–south transect is presented. North–south transects are well suited to study the surface movement in the Campine coal district, as the mined area forms a relatively narrow band orientated in the east–west direction [18]. Data were acquired for research through a European Space Agency (ESA) research proposal [4], i.e., the European C-band ERS1/2 data and the ENVISAT-ASAR data, respectively. Figure 1a presents the total uplift occurring in the period from October 1992 (i.e., moment that uplift was clearly visible) through December 2000 (i.e., end of the monitoring period). Figure 1b covers the period from December 2003 through September 2010. Along this transect, the longwall panels were mined between the north–south coordinates of 0.0 km and 5.25 km (indicated by blue square dotted lines), and the central shafts were situated around 4.1 km (shown by purple square). During the first 8 years of uplift (Figure 1a), the overall shape of the uplift curve is an inverse trough, with the largest values between north–south coordinates of 2.5 to 4.0 km. This zone is situated south of the central shafts position. It is situated more to the north than the middle of the mined zone. During this period, the maximum amount of uplift measured is about 175 mm (average maximum uplift rate of about 22 mm/year). Both to the north and to the south of the mined zone, uplift clearly is observed. At the southern and northern limit, about 75 mm and 125 mm are measured during the 8-year period, respectively. The extent of the zone with clear uplift is about 3 km to the north and south of the mined boundaries.

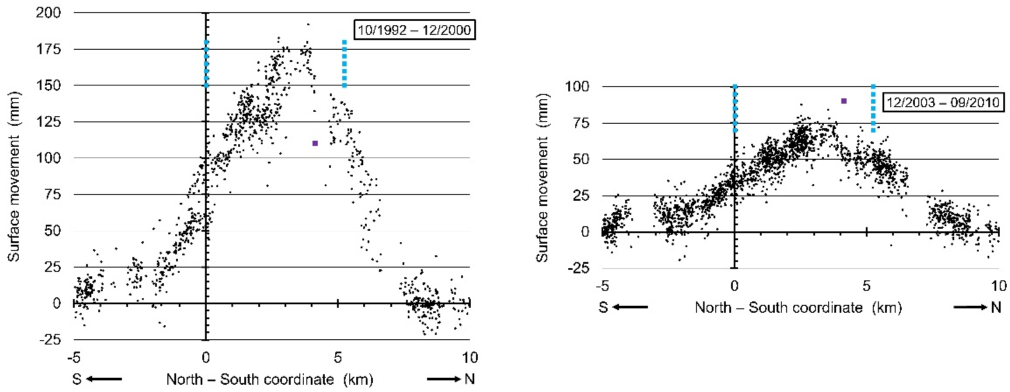

(**a**) (**b**)

Figure 1. Variation of the uplift along a north–south transect, above the coal mine of Eisden, Belgium: (**a**) From October 1992 through December 2000; (**b**) From December 2003 through September 2010. Along this transect, the mining took place between 0 and 5.25 km (blue square dotted lines). The position of the central shafts is indicated by purple square (north–south coordinate of 4.1 km).

During the second observation period (Figure 1b), the additional uplift curve has also an inverse trough shape. The maximum values occur approximately at the same north–south coordinates. However, the maximum average uplift rate is smaller, i.e., about 10 mm/year (a total maximum additional uplift of about 70 mm over 6 years and 9 months). The uplift zone also is further extended to the south and the north, and it covers now a zone of 4 to 5 km.

In [17], an analytical framework is presented and applied. (See reference for all details and a systematic discussion of the various parameters selected and their values chosen.) It shows a good correlation with the measurements along the north–south transect, which is also discussed in this paper. This framework was also applied successfully for other case studies [12,19,20]. The basic reasoning is that mining results in a drainage of pore water in all strata with mining activities, i.e., in and around the mine infrastructure and the goaf volumes, but also in the fractured and deformed rock mass, e.g., between the different seams mined. Note that at a specific location, five to 10 seams are sometimes mined within a depth interval of several hundred meters (see further). Once the underground pumping is stopped, the hydraulic pressure starts to increase until the original hydraulic gradient is re-established. The latter is on average a linear increase in the pore pressure as a function of depth, with a zero pressure at or close to the surface (see further for details). The increase in the water pressure during the flooding leads to a decrease in the effective stresses as the total stresses remain constant. This leads to an expansion of the rock material, and this expansion is transferred to the surface. The analytical approach allows the investigation of the impact of different parameters and parameter values on the uplift values in a comparatively easy way. For example, the impact of the expansion of the goaf volume only can be investigated without considering the expansion of other rock volumes (and vice versa). In a similar easy way, the hydraulic pressure distribution at the end of the mining phase can be changed, or only the stiffness values of the intact strata can be increased, etc. By analyzing many different options, it is possible to gain an understanding of how the various parameters impact the uplift. Satisfactory results are obtained when (i) the changes in pore pressure or water pressure, due to drainage, in the entire mined volume and in the surrounding rock mass are considered, and (ii) not only the expansion of the goaf volumes due to the fluid pressure being restored is considered but also the expansion of the rest of the strata layers, i.e., the non-collapsed strata layers. The complex mining geometry in the Campine coal district is an advantage to evaluate the impact of the various components.

As for the measurements, 2D transects (north–south oriented) are considered. The proposed framework is an analytical approach, whereby the entire 2D north–south vertical section is divided in elements with a height of 50 m and a north–south length of 250 m. The depth of the entire model is extended just below the deepest longwall panel. Each element expands when the pore pressure is increased. This expansion is assumed to take place at the center of each element. A transfer function based on the Boussinesq formula for a line load is applied to translate the expansion of an underground element on the movement of the earth surface. Here, an angle of influence of 45° is applied. The vertical stiffness of each element takes the real composition of each element into account, i.e., the thickness of the goaf volume of each longwall panel in an element and the thickness of the other non-collapsed strata within the element height of 50 m. By an increase in fluid pressure and considering the average vertical stiffness, the expansion of each element is estimated. Basic elastic equations are used that consider the impact of a change in effective stress on the vertical expansion. For each node at the surface, the sum is made of the impact of all elements in the underground. Each element with one or more longwall panels is composed of goaf volume(s) and of broken and/or deformed strata, i.e., the non-collapsed strata layers. The average stiffness ratio of the latter vs. the goaf material is assumed to be 10 to 1 for the basic case. The absolute values are 2 and 0.2 GPa, respectively (Poisson's ratio equal to 0.25). In the approach described in [17], there was no attempt to try to determine the various values by back-analysis. Rather, the values were determined by logical reasoning.

3. Framework for Different Hydrogeological Conditions

3.1. Original Applied Framework

The basic approach in the original applied framework [17] is that the end of the mining phase is characterized by a lower water pressure within an envelope around all mined longwall panels along a 2D north–south transect (Figure 2). Each longwall panel along the north–south transect studied is indicated by a short black line. The largest number of panels was mined between the north–south coordinates of 2.50 to 3.75 km. The dip to the north of the strata is clearly visible in this figure. The best results, in comparison to the measurements, are obtained when the drained zone is extended over 1 km to the north and to the south of the mined zone [12,17,19]. The good correlation with the measurements is observed for both the shape of the calculated uplift variation along a north–south transect and for the absolute maximum uplift value. The proposed water pressure distribution assumes that the excavations and the goaf volumes induce a drainage in all the strata layers within the entire volume with mining activities, i.e., in the excavations and goaf, but also outside the goaf volumes. However, it is not assumed that full drainage (i.e., zero water pressure) occurs over the entire height of the drained strata. Some rock volumes, e.g., very low permeable strata, are not subjected to full drainage and at the end of the mine life, the pore pressure is, at least partly, re-established in the oldest part of the mine, which is situated at the top of the volume with mining activities. This reasoning, supported by the measurements of [21,22], results in a linear decrease in the average water pressure from the top to the bottom of the enveloping line (Figure 3a). The thick blue line is the original hydraulic gradient. It is also the final situation, i.e., when the underground is again fully flooded. The hydraulic pressure at the end of the mining phase is presented by the thick brown line. At the top, it is assumed that the original hydraulic pressure already has been re-established at the end of the mining phase. Above this depth, the original hydraulic gradient also is observed. At the bottom, where the most recent mining took place, the water pressure is assumed to be zero. Note that this linear decrease presents the average variation as a function of depth over discretized elements of 50 m on 250 m.

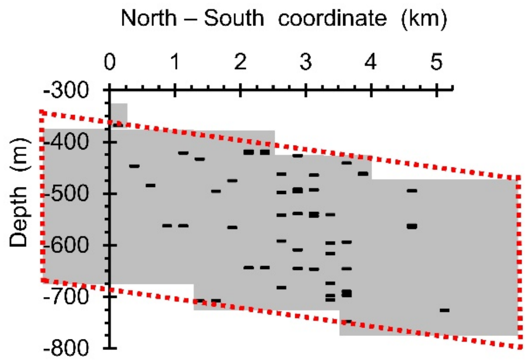

Figure 2. Illustration of the basic 2D model: envelope around all mined longwall panels (indicated by short black lines), including an extension of 1 km to north and to south, with a lower water pressure. The red dotted line follows the average dip of the strata. The gray shaded area is the discretization of the envelope, taking the dimensions of each element into account, i.e., a height of 50 m and a north–south length of 250 m.

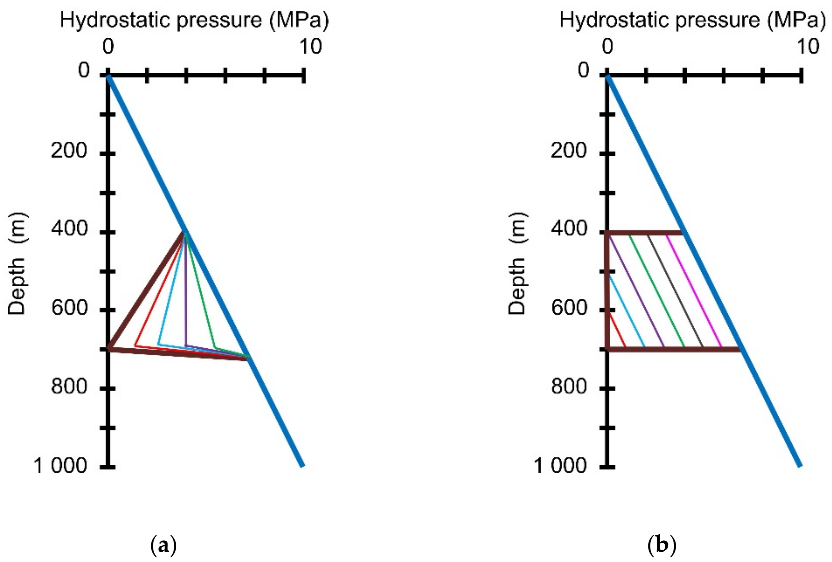

Figure 3. Variation of the water pressure as a function of depth for the situation that along this line the top longwall panel is situated at a depth of 400 m and the bottom panel at a depth of 700 m: (**a**) based on the approach in [17]; (**b**) adapted from the conditions presented in [23,24].

Although a variation as a function of time was observed, this variation was not studied in the original analytical framework published in 2021 [17]. The conditions at the start of the flooding (or at the end of the mining phase) were compared to the final situation (i.e., rock volume fully saturated again). For this paper, the increase in water pressure over time is presented in Figure 3a by the thinner lines. Over time, the change from the top panel depth downwards remains linear.

3.2. Alternative Hydrogeological Conditions

At the end of 2021, two papers were published, covering the same topic [23,24]. Their estimations are based on numerical simulations (using the FLAC3D-code). The pore pressure distribution at the end of mining and the increase in pore pressure during flooding are different from the one applied in [17]. As mentioned above, the proposed analytical framework allows in a relatively easy way the calculation of the impact of a change in a single parameter. Therefore, the hydrogeological assumptions, applied by Zhao and Konietzky [23,24], are integrated into the case study of Eisden colliery. All other properties and assumptions of the original framework [17] remain the same. The mining geometry of the simulations by Zhao and Konietzky was not used as input in the analytical framework, as their mining geometry only consisted of one or of two mined longwall panels in their fictitious abandoned coal mine. The latter is very different from the complex mining geometry of a real deep coal mine, such as for example the coal mine of Eisden.

The aim of introducing different hydraulic variations over the strata with mining activities is to evaluate if they could provide better results for the case study of the coal mine of Eisden. As the variations, presented in [23,24], are only applied on a simplified mining configuration of one or two longwall panels, some extrapolation is needed between their configuration and a real mine.

First, the authors [23,24] make a distinction between confined and unconfined mine water. Confined means that the volume above the goaf is impermeable, while unconfined means that the volume above the goaf is considered as permeable. Earlier research clearly showed that the expansion of the goaf volume only due to a change in water pressure does not provide realistic estimations of the uplift in the Campine coal basin [17]. This is in fact the reason why the shapes of the variations of (residual) subsidence vs. of uplift along north–south transects are different [11,18]. Subsidence is mainly triggered and induced by the roof collapse in the goaf volume, while the process of uplift is more complex. So, except to illustrate this point (see further), the expansion of the goaf volumes only is not considered in this paper.

Second, the authors [23,24] assume that the entire coal-bearing strata volume is completely drained and is characterized by a zero-water pressure at the end of the mining phase. The authors assume that underground pumping facilities create this condition. This is implemented into the analytical framework for evaluation and comparison purposes (see Figure 3b, thick brown line). However, I have my doubts if this scheme is realistic. In all deep coal mines that I have visited, there is always some water seepage and water flow, which means that there is some water and water pressure differences in the surrounding volume. It is not because for example in the shaft or tunnel, there is a zero-water pressure that further away from these openings there also is no water pressure. It is only in very extreme geological and hydrogeological circumstances that I can imagine such a zero-water pressure in the entire coal-bearing strata volume, e.g., for shallow mining, seams and coal strata outcropping in hills, no shale (or other low permeable) strata, etc. In [24], one of the models (confined) presents an impermeable layer of 50 m thick above the goaf, which is characterized by a zero-pore pressure. Again, in general terms, this seems to be unrealistic. An impermeable layer does not mean that it does not contain water and, hence, that it is characterized by a zero-pore pressure. This is clearly illustrated by measurements in the deep and thick layer of the Boom clay, which is a possible host rock for nuclear waste disposal [25,26]. Hence, the zero-pore pressure in impermeable layers is not integrated into the analytical calculations presented in this paper.

Third, the authors [23,24] assume that the entire volume fills up like an open reservoir. I have translated this by the successive thin colored lines in Figure 3b. They also consider various sources for the water inflow (from bottom, from sides and from above). In this and previous approaches, I have not really made this difference. For the Campine basin, I assume that there is water flow (i) from the south following the permeable strata layers, (ii) from above along permeable faults, induced fractures, and openings, and (iii) from below, as there is a pore pressure difference (e.g., between the deeper strata and the lowest mine level). However, this is not implicitly integrated in the proposed framework.

Fourth, the authors [23] consider two situations for the horizontal connections between the two goaf volumes considered, i.e., isolated vs. connected ponds. Furthermore, I only present results for the latter. For these so-called connected ponds, I assume that first (e.g., the first 50 m of water column), all elements situated between 725 and 775 m are filled. These elements are situated in the northern part only of the mined volume (north of 3.5 km in Figure 2). For the next 50 m of water, all elements between 675 and 725 m are filled additionally, and the water pressure below 725 m is further increased (see thin lines in Figure 3b). So, in this step, only the element columns south of the 1.25 km coordinate are still completely dry. The situation, which Zhao and Konietzky [23] call isolated ponds, is similar to the original analytical framework [17], but the reasoning behind the latter scheme is not that these columns would be isolated from each other, but that the flow along the dip of the strata plays a role.

4. Comparison of Impact of Hydrogeological Conditions and Their Variation as a Function of Time

All estimations are compared to the individual InSAR measurements along a north–south transect (see [1]). The time series of the European C-band ERS1/2 and of the ENVISAT-ASAR satellites are used. Past analyses have shown that these data are accurate (e.g., [1,3]) and that they provide an important source of information, which can never be realized by conventional leveling techniques. Both the spatial frequency, as the frequency as a function of time, are some orders larger than for the conventional leveling techniques. There is a spatial variation in the uplift and a variation of the uplift rate as a function of time, as illustrated in Figure 1. Therefore, three periods are selected, and the uplift occurring per time period is presented along the same north–south transect (Figure 4). The first time period (Figure 4, left column; from October 1992 through April 1995) is only 2.5 years long and covers the beginning of the uplift phenomenon. The coal mine was abandoned in 1988, which was followed by a short period of residual subsidence. The second and third time periods are 5 years long (Figure 4, middle and right column; from December 1995 through December 2000, and from September 2005 through September 2010, respectively). They both are situated at the end of each time series.

On the various graphs, the limits of the mined zone for this north–south transect are again indicated by blue square dotted lines, respectively, at a north–south coordinate of 0.0 and 5.25 km. The three rows of graphs in Figure 4 represent three different moments of additional water pressure in the rock mass, referring to the pressure at the bottom (a depth of 775 m). The top row represents the start of the flooding, i.e., the increase in water pressure from 0 to 1 MPa at the bottom. The middle row represents the increase from 2 to 3 MPa, and the bottom row rather is the situation at the end of flooding, i.e., from 5 to 6 MPa.

In the approach applied in [17], there was no attempt to try to determine the various values by back-analysis; rather, these values were determined by following a logical reasoning and by verifying afterwards whether a reasonable match is observed. For the latter, two criteria are used. First, the shape of the measured uplift is compared to the shape of the calculated uplift along a north–south transect. This is completed by presenting the values as a percentage of the maximum value. For the measured data, the maximum average value for the 250 m intervals is taken and not the individual maximum value. Second, the same order of magnitude of uplift should be obtained. As the process of uplift still carries on, the final uplift is unknown and can only approximately be estimated.

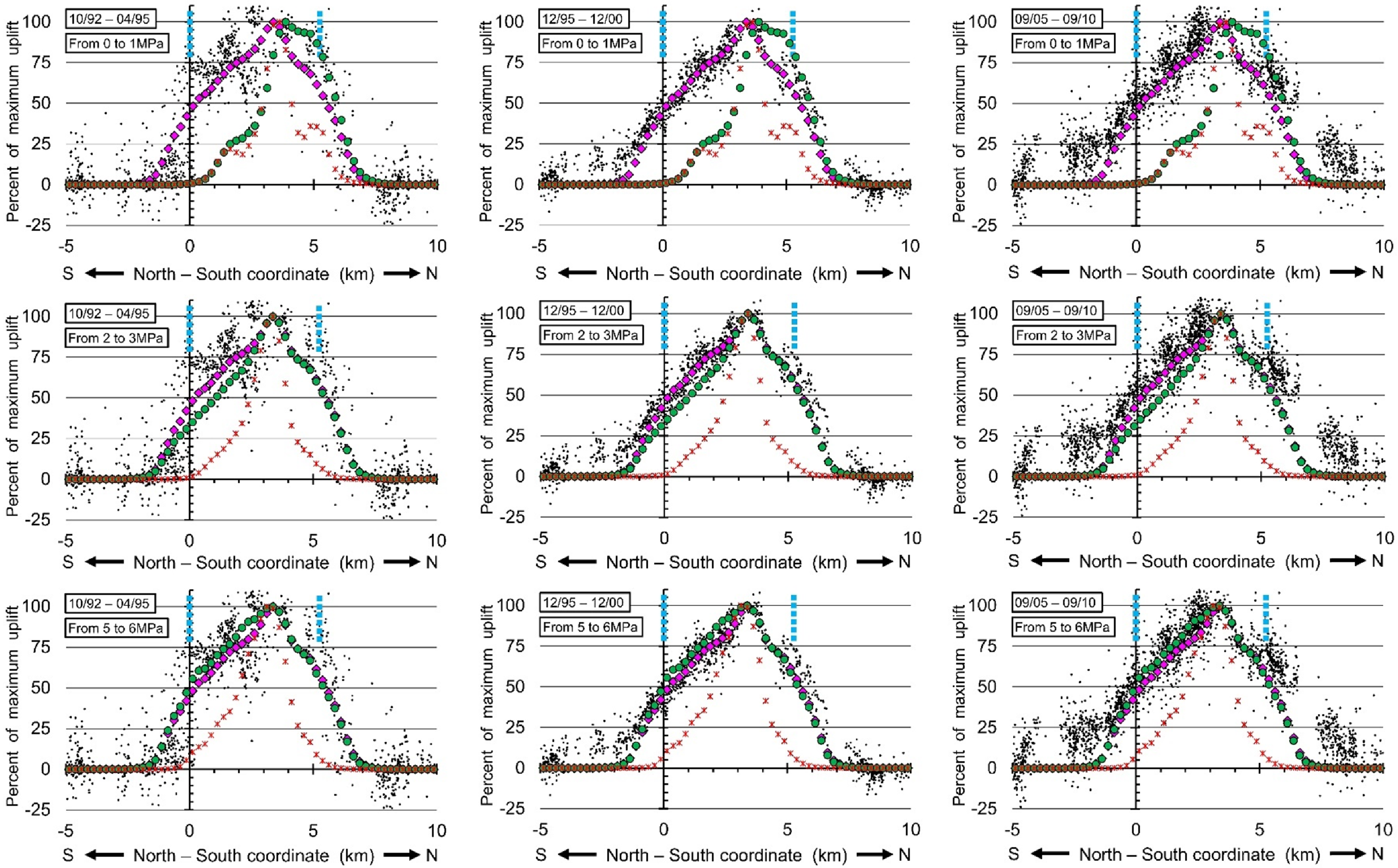

Figure 4. Comparison between InSAR data for three different time periods (black dots), estimations based on framework and property values presented in [17] (purple diamonds) and estimations for open reservoir scenario (green circles for contribution by goaf volume and strata surrounding mining activities, and red crosses for contribution by goaf volumes only). The three time periods are from October 1992 through April 1995 (left column), from December 1995 through December 2000 (middle column) and from September 2005 through September 2010 (right column). Three different increases in water height are presented (the same increase is presented per row; see labels and explanation in text). The limits of the mined area are indicated by blue square dotted lines.

4.1. Results for Framework Developed by Vervoort [17]

In Figure 4, the first set of calculations is based on all assumptions and property values presented in [17]. The situation, including the extension over 1 km to the north and to the south, as illustrated by the envelope in Figure 2, is presented by the purple diamond shapes. The change in hydraulic pressure as a function of time (or stage of flooding) is as illustrated in Figure 3a. The variation between the top and the bottom of the mined volume remains linear. As the values are presented as a function of the maximum additional uplift, this linear change results in the same shape of the calculated uplift curves for the three different moments in the flooding of the underground infrastructure and rock mass. Hence, as the shape of the measured values changes as a function of the moment in flooding, the estimated values for this type of variation is not optimal for the three increments of water pressure considered.

In [17], the results for the second time period (middle column in Figure 4) were presented and discussed in detail (purple diamond shapes only). As can be seen in Figure 4, in the middle column, a more than satisfactorily correlation is observed between the individual measurements, presented by the black dots, and the calculations, presented by the diamond shapes. In absolute terms, the maximum calculated uplift is 531 mm at 3.375 km, when comparing the initial water pressure distribution at mine closure with completely flooded situation (i.e., difference between thick brown and blue lines in Figure 3a). This value is slightly larger than the amount of uplift, which has been recorded to date, but the latter value is not the final value, as uplift still takes place. For the measurements, the largest values rather occur between north–south coordinates of 2.5 to 4.0 km. In other words, the calculated maximum is certainly situated within this zone. South of the maximum, the correlation with the individual measurements is very good above the mined zone. North of the maximum, the calculated values slightly underestimate the measured values. Further away than 1 to 2 km from the mined limits, the calculations still underestimate the measured values.

At the start of the uplift phase (Figure 4, left column), there is an underestimation of the measured values between the southern border of mining and the maximum of uplift (i.e., between a coordinate of 0 and 3 km). Outside the mined zone, there is an overestimation of the measured values toward the south but not toward the north. This is most likely linked to the spreading of the uplift process over time from the central area toward the mine borders and beyond, as illustrated in [1].

For the third time period corresponding to the later phase of the flooding (right column in Figure 4), there is an overall (small) underestimation over the entire length of the north–south transect.

In conclusion, the estimations based on a linear change of the water pressure as a function of depth provide a satisfactorily correlation with the measurements for the central period of the uplift process and thus of the flooding. At the start and toward the end of the flooding, the overall correlation remains acceptable, but the difference between measurements and calculations is larger. Most likely, this is rather linked to a change in extension to the north and to the south of the flooded area than to the assumed linear variation of the water pressure as a function of depth. For example, if at the start of the flooding, one would not already consider an extension to the south for the increase in water pressure, the overestimation to the south of the mined zone would be much smaller. In a similar way, a further extension of the envelope to the south, further than 1 km beyond the mined border, would decrease the underestimation in the last phase of flooding. These conclusions and reflections again indicate that the process of uplift is complex and that one is still in the phase of understanding this process. Therefore, it is worthwhile to consider other hydraulic assumptions.

4.2. Impact of Filling up Open Reservoir, Starting from Zero Water Pressure in Reservoir

One of the suggestions by [23,24] is that there is a zero-water pressure at the end of the mining phase in the mined volume (goaf volume only, or goaf, plus surrounding strata). One of the problems I was confronted with is how to best extrapolate the approach by [23], which was explained for a fictitious and unrealistic mine geometry (a total of one, or maximum two mining panels in the entire mine), to a real mine lay-out. Here, the decision has been made to consider the same volume with a lower water pressure as applied in [17] (see envelope in Figure 2), but that this volume has a zero-water pressure at the end of the mining phase (Figure 3b). It is also assumed that the scenario is applied, which Zhao and Konietzky [23] call a connected situation. In other words, we assume that during the filling of this open reservoir, first, the volume between a depth of 775 and 725 m is filled, second between 725 and 675 m, etc. (see thin lines in Figure 3b). For the calculations presented in Figure 4 (green circles), all other parameters are the same as for the purple diamonds, e.g., extension of drained zone to the north and to the south over 1 km, the same ratio goaf vs. coal-bearing strata, same moduli, etc.

In Figure 4, the additional uplift of both the surrounding strata and the goaf volumes is presented by green circles, while the component of the goaf volumes only is presented by red crosses. In addition, the latter is presented as a percentage of the maximum uplift due to the goaf volumes only. For the initial increase in water height (from a depth of 675 to 775 m; top row in Figure 4), the estimated uplift values show an extremely skewed shape along the north–south transect. This case should give the best correlation with the measurements of the first time period (from October 1992 through April 1995; left column in Figure 4). It is clear that over the entire length south of the maximum, the calculated values heavily underestimate the measurements. The calculated skewed shape is far from realistic. However, north of the maximum, the estimation is closer to the measurements. For a further increase in the water level from 200 to 300 m (middle row in Figure 4), in comparison to the deepest point at 775 m, the estimated curve for the open reservoir approaches the results in [17] and thus the measured values. The underestimation in the southern half is still present, but it is much smaller. For the last increase in water level presented (from 500 to 600 m; Figure 4 (bottom row)), the differences, south of the maximum, are similar between both estimations. However, now, the values for the open reservoir are larger than for the proposed conditions in [17].

If one would consider the expansion of the goaf volumes only (see curves with the red crosses in Figure 4), the differences between the measurements and the estimations are extremely large. It shows that integrating the goaf volumes only into a model cannot lead to realistic results. A change in the values of the goaf properties (i.e., height, stiffness, etc.) does not improve the estimated shape. It only influences the absolute values (e.g., the maximum). This confirms earlier findings [1,11,18,27,28], i.e., the process of subsidence, triggered by the roof collapses and correlated to the goaf height and composition, is different from the process of uplift, whereby re-establishing the hydraulic gradient in the non-collapsed coal-bearing strata plays a role, too. That is the reason why there is no direct correlation between the (residual) subsidence and the uplift [11,18] (see also Discussion and Conclusions below).

To illustrate that the difference between the framework developed in [17] and the open reservoir assumptions, based on [23,24], is not due to the different stiffness values in both models, a calculation is made for the stiffness values in [23,24]. As example, the combination of the second time period (from December 1995 through December 2000) with an increase in water height from 200 to 300 m is studied. This comparison is presented in Figure 5. Their elastic bulk (K) and shear (G) moduli for goaf (i.e., 0.83 GPa and 0.18 GPa, respectively) and for strata (i.e., 15.6 GPa and 7.6 GPa, respectively) correspond to a Young's moduli of 1.25 GPa and 23.33 GPa, respectively (if one assumes a Poisson's ratio of 0.25). The values applied in Figure 4 are 0.2 and 2 GPa, respectively. The way that the latter values were determined is discussed in detail in [17]. It was not by back-analysis, but, rather, determined by following a logical reasoning and basic rock mechanical knowledge.

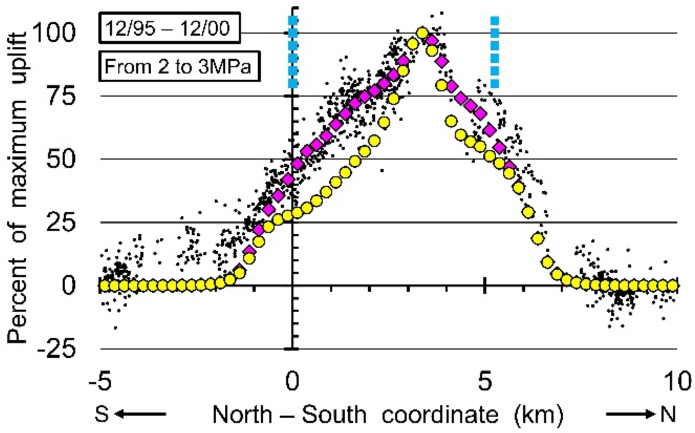

Figure 5. Comparison between InSAR data for the 5-year period from December 1995 through December 2000 (black dots), estimations based on framework and property values developed in [17] (purple diamonds) and estimations for open reservoir scenario and for moduli, as applied by numerical models in [23,24] (yellow circles), whereby the water column changes from 200 to 300 m. The limits of the mined area are indicated by blue square dotted lines.

Note that the combination presented in Figure 5 corresponds to one of the combinations closest to the measurements in Figure 4. While this combination for an open reservoir still provided a reasonable approximation of the measurements, the change in stiffness values certainly does not improve the approximation. There is now a larger under-estimation of the measured values over most of the mined zone. The reason is not so much linked to the absolute values of the stiffness but to the relative increase in the moduli ratio strata vs. goaf (from 10 on 1, to 18.7 on 1). In other words, the relative impact of the goaf has become larger and, as illustrated above, the contribution by only the goaf component is not a good approach. The total additional uplift in this phase is only 11.4 mm for the changed stiffness properties. For the original framework, an increase in the water pressure from 2 to 3 MPa resulted in an additional uplift of 68.5 mm. For the situation presented in Figure 4 (central graph), i.e., an open reservoir with same properties as in the original framework, the additional uplift is 94.9 mm. The contribution by the goaf volumes only is less than half, i.e., 44.3 mm.

4.3. Relation between Increase Water Pressure and Uplift

Various researchers have observed that there is a linear relation between the observed water level and the measured uplift (e.g., [3]). Note that the increase as a function of time is not linear, both for the water level, as the uplift. After a certain time, the rate decreases. This is also observed in the case study discussed in this paper (Figure 6). The variation of the uplift is presented as a function of time from August 1992 onwards over a period of 20 years based on InSAR data. The mean curves are presented for 10 reflectors closest to a central point. Three points are considered, i.e., at a north–south coordinate equal to 0.625 km, to 3.375 km (close to the maximum uplift) and to 4.625 km. The two outside locations are approximately at the same distance from the mined limits. Note that the values for 20 years are not the final values of uplift, as today (again 10 years later), the earth surface is still moving upwards. As mentioned above, there is no data for the change in water level in the Campine coal basin.

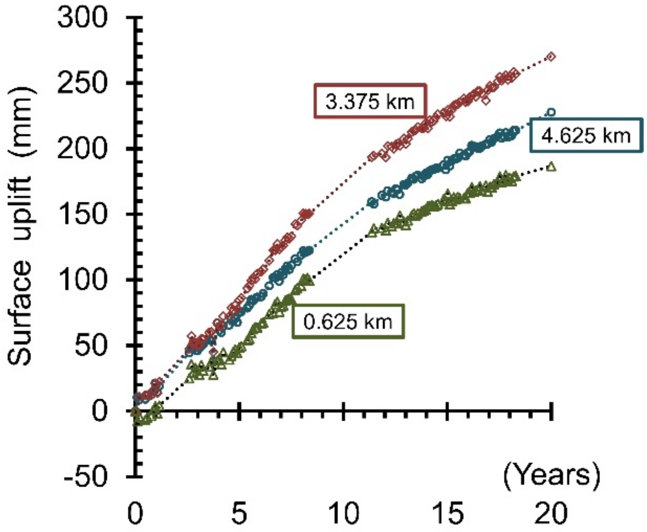

Figure 6. Variation of the uplift as a function of time from August 1992 onwards over a period of 20 years based on InSAR data. The mean curves are presented for 10 reflectors closest to a central point: green curve around a north–south coordinate equal to 0.625 km, burgundy curve around 3.375 km, and blue curve around 4.625 km.

In Figure 7, the relation between water level and uplift is presented for both sets of calculations. The increase in uplift at a north–south coordinate of 3.375 km (the location of the maximum uplift) is expressed as a percentage of the maximum calculated value at that location. For the framework developed by [17], the increase in water pressure corresponds to the change in pressure at a coordinate of 3.375 km. At that location, the depth of the bottom element is 725 m. In other words, the maximum (100%) is reached for 7.25 MPa. For the situation corresponding to an open reservoir, the increase in water pressure refers to the deepest point of the reservoir, i.e., a depth of 775 m in the northern part of the mined area. In other words, the maximum (100%) is reached for 7.75 MPa. As mentioned earlier, the relation for the original framework is linear (Figure 7, purple diamonds). The one corresponding to an open reservoir is not linear (Figure 7, green circles).

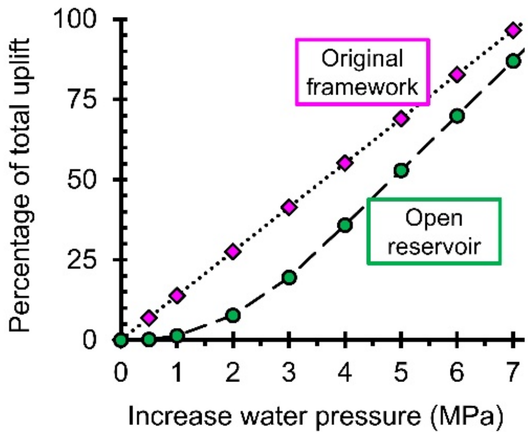

Figure 7. Relation between the amount of uplift at a north–south coordinate of 3.375 km and the increase in water pressure. The uplift is presented as a percentage of the maximum calculated amount of uplift at 3.375 km. The relation for the framework developed in [17] is presented by purple diamonds, and the model assuming an open reservoir is presented by green circles.

For both cases, the variation of the calculated uplift (absolute values) as a function of the increase in water pressure is presented in Figure 8. The movements at the three locations of Figure 6 are provided. For the original framework (Figure 8a), a linear relationship is observed as a function of the increase in water pressure. For the situation of an open reservoir (Figure 8b), the relation is not linear, also for a location (e.g., at 4.625 km) in the deepest part of the mine.

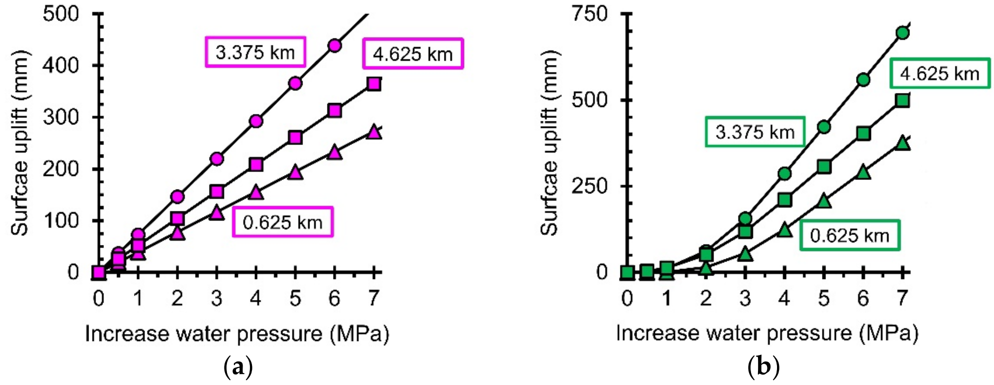

Figure 8. Variation of the amount of uplift as a function of the increase in water pressure: (**a**) The original framework developed in [17]; (**b**) The model assuming an open reservoir. Information is presented for three north–south coordinates: triangles presenting the coordinate of 0.625 km, circles 3.375 km and squares 4.625 km.

5. Discussion and Conclusions

The least one can conclude is that these additional calculations confirm that the process of uplift is an extremely complex process. There are still many unknowns, and one should not underestimate the process. I remain critical to researchers who are over-enthusiastic over the results of a numerical model and over the capability to predict future movements. I consider the analytical framework developed earlier [17] as a step in trying to better understand the full process and not yet a tool to predict uplift values in future projects. In addition, many years were spent to interpret in detail real and numerous measurements of this phenomenon, above several coal mines in the Belgian Campine coal district. These interpretations show the complexity of the process, with a variation of uplift values in time and space (e.g., [1]). The large number of InSAR measurements formed the basis to evaluate the results of the analytical framework. The frequency of measurements as a function of time is high, as is the amount of data points in an area with buildings and infrastructure. The analysis of these data needs of course the necessary experience and knowledge, and a good analysis is time consuming.

A first practical conclusion of the calculations presented in this paper is a confirmation that considering the expansion of the goaf volumes only does not lead to realistic results. If only the expansion of the goaf is included in the model, a change in stiffness of the goaf material or a change of the height of the collapsed volumes does not improve the results. The complex mining geometry in the Belgian Campine coal district allows a correct analysis of various contributions and their impact on the uplift. However, if the geometry would be limited to single seam mining or that everywhere, the same seams would be mined at the same depth and with the same thickness, a model incorporating the goaf volumes only could lead to the impression that reasonable results are obtained, but it would mean that the other aspects of the uplift process are not considered. This is the reason why there is no direct correlation between (residual) subsidence and uplift [11,18]. In addition, there is no direct link between the uplift and the mining characteristics. The total thickness of the strata with mining activities (i.e., between top and bottom longwall panel) is also important, and the expansion of this volume due to a change of pore pressure is an important part in the total uplift. Hence, the shape of the uplift curve along a north–south transect is the sum of the shapes of the expansion of the volume of the strata between goaf volumes and of the goaf volumes. As clearly illustrated by the transects above (i.e., Figures 4 and 5), it is not so that when the maximum of the contribution by the goaf only vs. the contribution by the rest of the strata are situated at about the same location, the full shape over the entire transect is the same for both contributions.

A second conclusion is related to the different possible distributions of the hydraulic pressures at the end of the mining phase. In the framework developed in [17], a linear trend is assumed for the average water pressure between the top longwall panel and the bottom one along a vertical line (Figure 3a). The suggestion by [23,24] is different, and they assume that there is a zero-pore pressure in the volume surrounding the mining activities at the end of the mining phase. This would be correct if one investigates open excavations, but I have my doubts if a zero-water pressure would ever be observed in the entire rock mass surrounding longwall panels. It would mean that there is no water at all and no water flow in that rock mass. Except maybe for a very particular geological and hydrogeological mining environment, it is not typical for the deep coal mining environment in Europe. The fact that they assume a zero-water pressure in the impermeable layers creates doubt that their starting hydraulic properties are correct, even that they are realistic. To be able to analyze their assumptions, I have assumed that the same volume of lower pore pressure (see envelope in Figure 2) has a zero-water pressure, and that this volume is filled by water as an open reservoir would be filled (Figure 3b). When starting to fill from the deepest part upwards, similar to an open reservoir, the induced uplift values result in a very skewed shape along north–south transects, which is significantly different from measured shapes at the start of the uplift phase. Note that all other characteristics and assumptions were the same as in the original developed framework [17]. This observation should be sufficient to put a question mark next to the scenario, which is called by [23] the connected case. At least, this question mark is justified for most deep coal mining conditions. For this scenario, the relation between uplift and water pressure increase is non-linear, while several researchers have measured a linear relationship (e.g., [3]). The latter is observed for the original framework developed in [17]. Zhao and Konietzky [23] also consider a scenario which they call isolated longwall panels, whereby the filling up of each mined and collapsed volume occurs independent of the neighboring volumes. The difference with the results of the original framework is smaller, but a non-linear relationship remains between uplift and water pressure. So, the least one could conclude is that the hydrogeological assumptions and their variation, as suggested by Zhao and Konietzky [23], are not better alternatives for the assumptions in the original framework. As mentioned above, I have my doubts if these alternatives are realistic for most deep coal mines. At the end, I want to stress that, more important than the choice between a modeling method (e.g., elastic equations, analytical calculations, finite element and finite difference method), one should make correct assumptions which form the input of all these methods.

For the final conclusion of this paper, I would like to repeat a quote out of [17]: "Although a reasonable match is realized between measurements and calculations, the developed framework cannot be considered to be final. Advanced hydrogeological modeling could lead to some more information about the distribution of the water pressure at the end of the mining period and, more specifically, the extent of the drained area." However, the latter will not be simple, as very little information is available on the state of the entire rock mass and on the hydrogeological conditions.

Funding: This research received no external funding.

Informed Consent Statement: Not applicable.

Conflicts of Interest: The author declares no conflict of interest.

References

1. Vervoort, A. Uplift of the surface of the earth above abandoned coal mines. Part A: Analysis of satellite data related to the movement of the surface. *Int. J. Rock Mech. Min. Sci.* **2021**, *148*, 104896. [CrossRef]
2. Baglikow, V. Damage-relevant effects of mine water recovery—Conclusions from the Erkelenz hard coal district. *Markscheidewesen* **2011**, *118*, 10–16.

3. Caro Cuenca, M.; Hooper, A.J.; Hanssen, R.F. Surface deformation induced by water influx in the abandoned coal mines in Limburg, the Netherlands observed by satellite radar interferometry. *J. Appl. Geophys.* **2013**, *88*, 1–11. [CrossRef]
4. Devleeschouwer, X.; Declercq, P.Y.; Flamion, B.; Brixko, J.; Timmermans, A.; Vanneste, J. Uplift revealed by radar interferometry around Liège (Belgium): A relation with rising mining groundwater. In Proceedings of the Symposium Post-Mining 2008, Nancy, France, 6–8 February 2008.
5. Gee, D.; Bateson, L.; Sowter, A.; Grebby, S.; Novellino, A.; Cigna, F.; Marsh, S.; Banton, C.; Wyatt, L. Ground Motion in Areas of Abandoned Mining: Application of the Intermittent SBAS (ISBAS) to the Northumberland and Durham Coalfield, UK. *Geosciences* **2017**, *7*, 85. [CrossRef]
6. Herrero, C.; Muñoz, A.; Catalina, J.C.; Hadj-Hassen, F.; Kuchenbecker, R.; Spreckels, V.; Juzwa, J.; Bennett, S.; Purvis, M.; Bigby, D.; et al. *Prediction and Monitoring of Subsidence Hazards Above Coal Mines (Presidence)*; RFCS Final Report RFCR-CT-2007-00004, EUR 25057 EN; European Commission: Brussels, Belgium, 2012.
7. Samsonov, S.; d'Oreye, N.; Smets, B. Ground deformation associated with post-mining activity at the French–German border revealed by novel InSAR time series method. *Int. J. Appl. Earth Obs. Geoinf.* **2013**, *23*, 142–154. [CrossRef]
8. Jirankova, E.; Konicek, P. Ground surface uplift during hardcoal longwall mining. *Int. J. Rock Mech. Min. Sci.* **2022**, *153*, 105099. [CrossRef]
9. Mehrabi, A.; Derakhshani, R.; Nilfouroushan, F.; Rahnamarad, J.; Azarafza, M. Spatiotemporal subsidence over Pabdana coal mine Kerman Province, central Iran using time-series of Sentinel-1 remote sensing imagery. *Epis. J. Int. Geosci.* **2022**, *2022*, 1–15. [CrossRef]
10. Vervoort, A. The Time Duration of the Effects of Total Extraction Mining Methods on Surface Movement. *Energies* **2020**, *13*, 4107. [CrossRef]
11. Vervoort, A. Long-term impact of coal mining on surface movement: Residual subsidence versus uplift. *Min. Rep. Glückauf.* **2020**, *156*, 136–141.
12. Vervoort, A. Impact of the closure of a coal district on the environmental issue of long-term surface movements. *AIMS Geosci.* **2022**, *8*, 326–345. [CrossRef]
13. Soltanieh, A.; Macciotta, R. Updated Understanding of the Ripley Landslide Kinematics Using Satellite InSAR. *Geosciences* **2022**, *12*, 298. [CrossRef]
14. Shang, H.; Zhan, H.Z.; Ni, W.K.; Liu, Y.; Gan, Z.H.; Liu, S.H. Surface Environmental Evolution Monitoring in Coal Mining Subsidence Area Based on Multi-Source Remote Sensing Data. *Front. Earth Sci.* **2022**, *10*, 790737. [CrossRef]
15. Alatza, S.; Papoutsis, I.; Paradissis, D.; Kontoes, C.; Papadopoulos, G.A.; Raptakis, C. InSAR Time-Series Analysis for Monitoring Ground Displacement Trends in the Western Hellenic Arc: The Kythira Island, Greece. *Geosciences* **2020**, *10*, 293. [CrossRef]
16. He, Y.; Wang, W.; Yan, H.; Zhang, L.; Chen, Y.; Yang, S. Characteristics of Surface Deformation in Lanzhou with Sentinel-1A TOPS. *Geosciences* **2020**, *10*, 99. [CrossRef]
17. Vervoort, A. Uplift of the surface of the earth above abandoned coal mines. Part B: Framework to understand and explain uplift. *Int. J. Rock Mech. Min. Sci.* **2021**, *148*, 104947. [CrossRef]
18. Vervoort, A. Surface movement above an underground coal longwall mine after closure. *Nat. Hazards Earth Syst. Sci.* **2016**, *16*, 2107–2121. [CrossRef]
19. Vervoort, A. Upward surface movement above deep coal mines after closure and flooding: Analytical modeling results. In Proceedings of the SME 2022 International Conference on Ground Control in Mining, Canonsburg, PA, USA, 26–28 July 2022. Paper 0601.
20. Vervoort, A. Challenge to explain the upward surface movement above abandoned coal mines. In Proceedings of the Geotechnical Challenges in Mining, Tunneling and Underground Infrastructures, ICGMTU 2021, Lecture Notes in Civil Engineering, Virtual, 20 December 2021; Springer: Singapore, 2021; Volume 228. [CrossRef]
21. David, K.; Timms, W.A.; Barbour, S.L.; Mitra, R. Tracking changes in the specific storage of overburden rock during longwall coal mining. *J. Hydrol.* **2017**, *553*, 304–320. [CrossRef]
22. Tammetta, P. Estimation of the height of complete groundwater drainage above mined longwall panels. *Groundwater (NGWA)* **2013**, *51*, 723–734, and comments by author on discussion, *Groundwater (NGWA)* **2014**, *52*, 339–342. [CrossRef]
23. Zhao, J.; Konietzky, H. An overview on flooding induced uplift for abandoned coal mines. *Int. J. Rock Mech. Min. Sci.* **2021**, *148*, 104955. [CrossRef]
24. Zhao, J.; Konietzky, H.; Herbst, M.; Morgenstern, R. Numerical simulation of flooding induced uplift for abandoned coal mines: Simulation schemes and parameter sensitivity. *Int. J. Coal Sci. Technol.* **2021**, *8*, 1238–1249. [CrossRef]
25. Barnichon, J.D.; Volckaert, G. Observations and predictions of hydromechanical coupling effects in the Boom clay, Mol Underground Research Laboratory, Belgium. *Hydrogeol. J.* **2003**, *11*, 193–202. [CrossRef]
26. Bernier, F.; Li, X.L.; Bastiaens, W. Twenty-five years' geotechnical observation and testing in the Tertiary Boom Clay formation. *Géotechnique* **2007**, *57*, 229–237. [CrossRef]
27. Vervoort, A.; Declercq, P.Y. Surface movement above old coal longwalls after mine closure. *Int. J. Min. Sci. Technol.* **2017**, *27*, 481–490. [CrossRef]
28. Vervoort, A.; Declercq, P.Y. Upward surface movement above deep coal mines after closure and flooding of underground workings. *Int. J. Min. Sci. Technol.* **2018**, *28*, 53–59. [CrossRef]